

Percolation thresholds on triangular lattice for neighbourhoods containing sites up-to the fifth coordination zone

Krzysztof Malarz*

*AGH University of Science and Technology,
Faculty of Physics and Applied Computer Science,
al. Mickiewicza 30, 30-059 Kraków, Poland*

(Dated: June 11, 2022)

We determine thresholds p_c for random-site percolation on a triangular lattice for all available neighborhoods containing sites from the first to the fifth coordination zones, including their complex combinations. There are 31 distinct neighbourhoods. The dependence of the value of the percolation thresholds p_c on the coordination number z are tested against various theoretical predictions. The newly proposed single scalar index $\xi = \sum_i z_i r_i^2 / \zeta_i$ (depending on the coordination zone number ζ , the neighbourhood coordination number z and the square-distance r^2 to sites in ζ -th coordination zone from the central site) allows to differentiate among various neighbourhoods and relate p_c to ξ . The thresholds roughly follow a power law $p_c \propto \xi^{-\gamma}$ with $\gamma \approx 0.705(23)$.

Keywords: random site percolation; triangular lattice; complex and extended neighborhoods; Newman–Ziff algorithm; Bastas *et al.* method; finite size scaling hypothesis; analytical formulas for percolation thresholds

I. INTRODUCTION

The concepts of site and bond percolation [1, 2] introduced in middle fifties [3, 4] and since then have been applied in various fields of science ranging from agriculture [5] via studies of polymer composites [6], materials science [7], forest fires [8], oil and gas exploration [9], quantifying urban areas [10], Bitcoins transfer [11], diseases propagation [12] to transportation networks [13] (see Refs. 14 and 15 for reviews).

Percolation is an example of phenomenon where a geometrical phase transition (on d -dimensional lattice) takes place. The critical parameter (called percolation threshold p_c [16]) separates two phases: one for a low occupation probability $p < p_c$ and the other for $p > p_c$. In the low- p phase the system behaves as an insulator (without connectivity path leading between system boundaries) while for the high- p phase there is a giant component spanning the system and connecting opposite boundaries; in effect the system behaves as a conductor, when one refers to the electric analogy.

The percolation thresholds were initially estimated for nearest neighbour interactions [17, 18] but later also complex (or extended) neighbourhoods were studied for 2D (square [19–25], triangular [19, 20, 26, 27], honeycomb [19]), 3D (simple cubic [25, 28, 29]) and 4D (simple hypercubic [30]) lattices.

Very recently, we have computed percolation thresholds for random site percolation on triangular lattice with complex neighbourhoods with hexagonal symmetry [27]. Here we supplement these results with 31 percolation thresholds estimations for all neighbourhoods on triangular lattice containing sites from the first, the second, the third, the fourth and the fifth coordination zones (see

Figure 1). Some of these neighbourhoods—those containing sites from the fifth coordination zone—are presented in Figure A1 in Appendix A. The lattice names follow convention proposed in Ref. 25 reflecting lattice topology (here TR, i.e. triangular lattice) and numerical string specifying the coordination zones ζ , where sites constituting the neighbourhood come from.

Additionally—for triangular lattice and complex neighbourhoods—we test the dependence of p_c on the coordination number z , following the idea of Ref. 25. However, instead of values of the percolation thresholds for selected (mainly compact) neighbourhoods, we use the mean values \bar{p}_c of percolation thresholds p_c averaged over all available neighbourhoods with given coordination number z . Unfortunately, values of \bar{p}_c do not follow any of dependencies proposed in Ref. 25.

Finally, we propose a scalar quantity ξ which may be helpful for differentiating among various neighbourhoods. The quantity is based on the coordination zone ζ , the sites number z and the sites distances r to the central site in the neighbourhood. The dependency of p_c on this newly proposed index ξ follows roughly a power law with an exponent close to $-0.705(23)$.

II. METHODS

In order to evaluate the percolation thresholds p_c we follow the scheme applied previously in Ref. 27. Namely, we combine Newman and Ziff [31], Bastas *et al.* [32] algorithms with finite size corrections [1, 33] to estimate p_c :

1. Based on the Newman and Ziff [31] algorithm we calculate the size of the largest cluster $\langle S_{\max} \rangle$ on the number of occupied sites n (Figure 2a). The brackets $\langle \dots \rangle$ represent averaging over $R = 10^5$ lattice realizations. Applying a Gaussian approxi-

*  0000-0001-9980-0363; malarz@agh.edu.pl

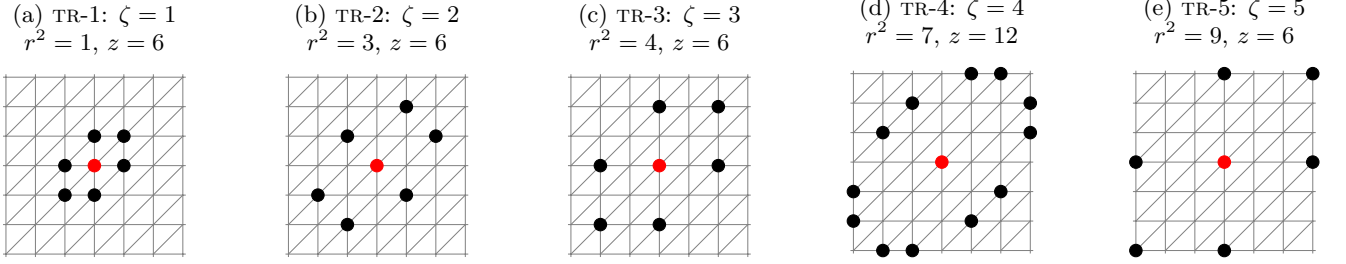


FIG. 1: (Color online). Basic neighbourhoods corresponding to subsequent coordination zones $\zeta = 1, \dots, 5$ on the triangular lattice. The symbol r stands for the Euclidean distance of black sites to the central one (in red) and z indicates the number of sites in the neighbourhood. Examples of fifteen neighborhoods containing the next-next-nearest-nearest neighbors (with sites from the 5-th coordination zone) on triangular lattice are presented in Figure A1 in Appendix A.

mation to the he Bernoulli distribution

$$\mathcal{S}_{\max}(n; N, p) = \binom{N}{n} p^n (1-p)^{N-n} \quad (1)$$

one can calculate \mathcal{S}_{\max} for different values of the occupation probability p using the Gauss function:

$$\mathcal{G}(n; \mu, \sigma) = \frac{1}{\sqrt{2\pi\sigma^2}} \exp\left(-\frac{(n-\mu)^2}{2\sigma^2}\right), \quad (2)$$

with the expected value $\mu = pN$ and variance $\sigma^2 = p(1-p)N$. The dependence $\mathcal{S}_{\max}(n; N, p)$ yields a probability of belonging to the largest cluster

$$\mathcal{P}_{\max} = \langle \mathcal{S}_{\max} \rangle / N, \quad (3)$$

for $N = L^2$ and $L = 64, 128, 256, 512, 1024, 2048$ and 4096 sites as presented in Figure 2b;

- Using Bastas *et al.* [32] algorithm we minimize the pair-wise difference

$$\lambda(p) = \sum_{i \neq j} [\mathcal{H}(p; N_i) - \mathcal{H}(p; N_j)]^2 \quad (4)$$

function (see Figure 2c) with $\mathcal{H}(p; L) = L^{\beta/\nu} \cdot \mathcal{P}_{\max}(p; L) + 1/[L^{\beta/\nu} \cdot \mathcal{P}_{\max}(p; L)]$ [34] and with exponents $\beta = \frac{5}{36}$ and $\nu = \frac{4}{3}$ [1, p. 54]. The minimum of $\lambda(p)$ estimates the percolation threshold \hat{p}_c ;

- Finally, in Figure 2d we plot the estimated values of percolation thresholds $\hat{p}_c(L)$ for different ranges of summation in Equation (4)—up to $L = \max(L_{i,j}) = 512, 1024, 2048$ and 4096. According to the standard finite size scaling [1, p. 77]

$$\hat{p}_c(L) = p_c + a \cdot L^{-1/\nu}, \quad (5)$$

where p_c is the percolation threshold for an infinitely large system. The least squares linear fit to data presented in Figure 2d predicts p_c and its uncertainty $u(p_c)$.

III. RESULTS

In Figure 2 we present examples of results used to predict the percolation thresholds p_c as described in Section II.

In Figure 2a the dependence of $\langle \mathcal{S}_{\max}(n; L) \rangle$ on the number of occupied sites n (normalized to the system size N) are presented. The dependence for all discussed neighbourhoods is presented in Figure A2 in Appendix A. With the increase of the system size $N = L^2$ the curves describing this dependence become steeper and steeper. For infinitely large systems the function $d\langle \mathcal{S}_{\max}(n; L) \rangle / dn$ becomes discontinuous at $p = p_c$.

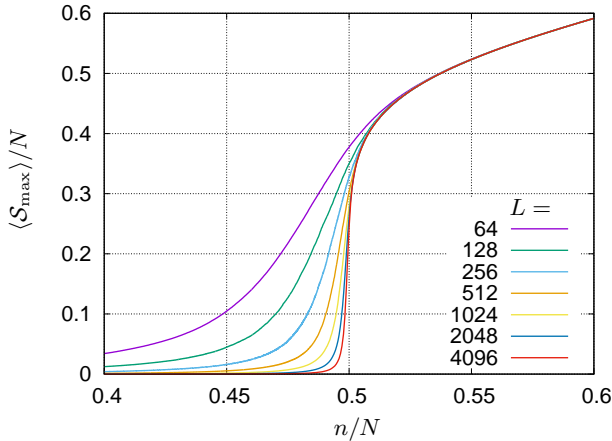
In Figure 2b we show the dependence of the normalized probability of belonging to the largest cluster $\mathcal{P}_{\max}(p; L) \cdot L^{\beta/\nu}$ on the sites occupation probability p for various linear system sizes L . The curves representing this dependence for all discussed neighbourhoods are presented in Figure A3 in Appendix A. The abscissas of the points where curves intercept each other estimate the percolation thresholds \hat{p}_c .

In Figure 2c the dependence of $\lambda(p)$ on the occupation probability p is presented. The curves representing this dependence for all discussed neighbourhoods are presented in Figure A4 in Appendix A. The minima of $\lambda(p)$ give estimates of the percolation thresholds \hat{p}_c .

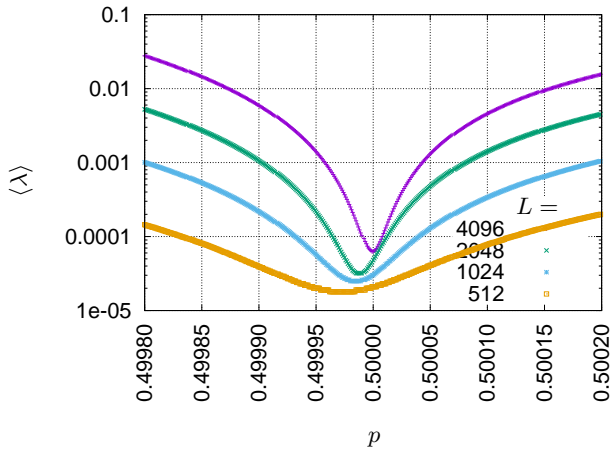
In Figure 2d finite size corrections to \hat{p}_c according to Equation (5) are presented. The curves representing this dependence for all discussed neighbourhoods are presented in Figure A5 in Appendix A. The initial value of the linear fit function predicts the percolation threshold values p_c .

The obtained percolation thresholds p_c together with their uncertainties and earlier estimates are gathered in Table I. We used all lattice sizes $64 \leq L \leq 4096$ for the estimation of p_c (they are collected in the sixth column of Table I), while estimations given in the fifth column rely on systems with $128 \leq L \leq 4096$ (i.e. the smallest systems, for $L = 64$, have been excluded from calculations). For neighbourhoods containing 30 or more sites we were able to carry out simulations for lattices up to

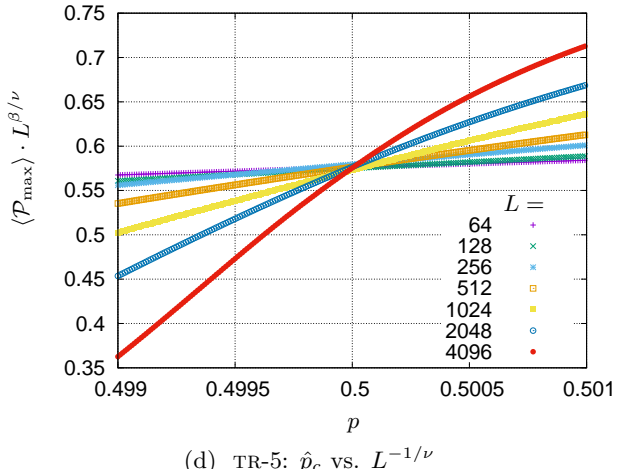
(a) TR-5: The mean largest cluster size $\langle S_{\max} \rangle$ vs. the number of occupied sites, normalized to the system size N



(c) TR-5: $\langle \lambda(p) \rangle$ vs. the occupation probability p



(b) TR-5: The probability of belonging to the largest cluster $\langle P_{\max} \rangle$ vs. the occupation probability p



(d) TR-5: \hat{p}_c vs. $L^{-1/\nu}$

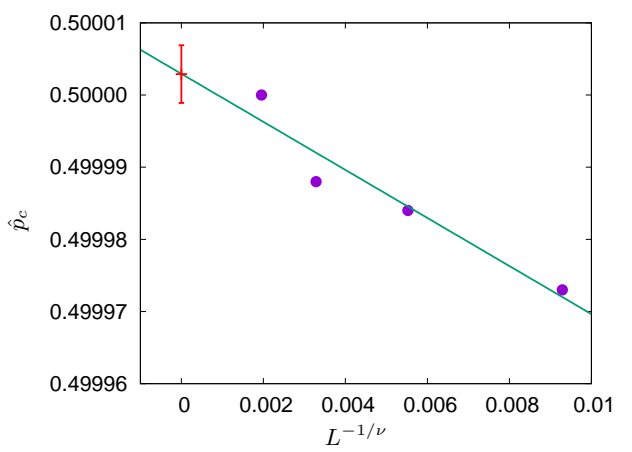


FIG. 2: (Color online). Subsequent steps of the percolation threshold estimation (example for TR-5 lattice). (a) The Dependence of $\langle S_{\max}(n; L) \rangle$ on the number of occupied sites n (normalized to the system size N). (b) The dependence of $\langle P_{\max}(p; L) \rangle \cdot L^{\beta/\nu}$ on the occupation probability p . (c) The dependence of $\langle \lambda(p) \rangle$ on the occupation probability p . The minima give estimates of the percolation thresholds \hat{p}_c . (d) Finite size-scaling corrections to \hat{p}_c according to Equation (5).

$L = 2048$. To check how the minimisation of pair-wise difference function λ (4) reduces the finite size effects we present also values of p for which λ reaches the minimum when p is scanned with $\Delta p = 10^{-6}$ accuracy (see the fourth column of Table I).

IV. DISCUSSION

In Ref. 25 several analytical formulas for the dependence of the percolation threshold p_c on the coordination number z were tested, with

$$p_c = c/(z + b), \quad (6)$$

$$p_c = 1 - \exp(d/z) \quad (7)$$

among the others. These formulas work fine for “compact” neighbourhoods (for instance TR-1, TR-1,2,3 and TR-1,2,3,4,5, here).

Unfortunately, for complex neighbourhoods these formulas must fail as the dependence p_c on z is “degenerated”, i.e. several values of p_c are associated with the same number z of sites in the neighbourhood (see Figure 3a, and also Figure 4b in Ref. 24 for the square lattice). These degeneration is also observed for basic neighbourhoods what brought some brickbats [35] on the possibility of existing universal formulas for the percolation threshold (depending solely on the spatial dimension d of the system and the coordination number z), as proposed in Galam and Mauger [36].

To remove this degeneracy we tested formulas (6) and (7) for the mean values \bar{p}_c of percolation thresholds. The averaging, denoted by the bar, goes over percola-

TABLE I: Estimated values of random site triangular lattice percolation thresholds p_c for various complex neighbourhoods. The lattice name encodes the coordination zones ζ , to which sites in the neighbourhood belong. Also the coordination number z , the index ξ and the value of p at the minimum of λ are presented.

lattice	z	ξ	p at $\min\langle\lambda\rangle$ ($128 \leq L \leq 4096$) with $\Delta p = 10^{-6}$	p_c ($128 \leq L \leq 4096$)	p_c ($64 \leq L \leq 4096$)	earlier estimations
TR-1,2,3,4,5	36	54.8	0.1157 40 ^a	0.1157370(74) ^a	0.1157399(58) ^a	0.115847(21) [27]
TR-2,3,4,5	30	48.8	0.1174 40 ^a	0.117467(15) ^a	0.117460(10) ^a	0.117579(41) [27]
TR-1,3,4,5	30	45.8	0.1215 48 ^a	0.121583(14) ^a	0.1215730(83) ^a	
TR-1,2,4,5	30	46.8	0.1225 93 ^a	0.1226215(68) ^a	0.1226119(30) ^a	
TR-1,2,3,5	24	33.8	0.1522 59	0.152297(17)	0.152282(10)	
TR-3,4,5	24	39.8	0.1255 48	0.1255511(43)	0.1255483(43)	
TR-2,4,5	24	40.8	0.1266 22	0.126653(11)	0.1266400(40)	
TR-2,3,5	18	27.8	0.1616 45	0.161664(15)	0.161653(15)	
TR-1,4,5	24	37.8	0.1316 69	0.1316677(13)	0.13166484(66)	0.131792(58) [27]
TR-1,3,5	18	24.8	0.1700 42	0.1700473(87)	0.170039(10)	
TR-1,2,5	18	25.8	0.1762 42	0.176263(11)	0.1762610(92)	
TR-4,5	18	31.8	0.1402 43	0.1402453(79)	0.1402382(92)	0.140286(5) [27]
TR-3,5	12	18.8	0.1957 03	0.1956981(14)	0.1957039(24)	
TR-2,5	12	19.8	0.2902 68	0.290280(20)	0.290279(17)	
TR-1,5	12	16.8	0.2095 62	0.209563(13)	0.209561(10)	
TR-5	6	10.8	0.5000 00	0.5000029(40)	0.4999961(55)	$\frac{1}{2}$ [27]
TR-1,2,3,4	30	44	0.1358 13 ^a	0.135817(29) ^a	0.135823(27) ^a	
TR-2,3,4	24	38	0.1391 15	0.1391118(33)	0.1391117(26)	
TR-1,3,4	24	35	0.1443 07	0.1443064(38)	0.1443074(32)	
TR-1,2,4	24	36	0.1489 78	0.1489791(88)	0.1489757(74)	
TR-3,4	18	29	0.1519 32	0.1519532(26)	0.1519393(35)	
TR-2,4	18	30	0.1584 53	0.1584634(54)	0.1584620(43)	
TR-1,4	18	27	0.1651 88	0.165186(14)	0.165186(12)	
TR-4	12	21	0.1924 37	0.1924356(68)	0.1924428(50)	0.192410(43) [27]
TR-1,2,3	18	23	0.2154 62	0.21546261(91)	0.2154657(17)	0.215484(19) [27], 0.215 [26]
TR-2,3	12	17	0.2320 12	0.232019(23)	0.232020(20)	0.232008(38) [27]
TR-1,3	12	14	0.2645 25	0.264545(25)	0.264539(21)	
TR-3	6	8	0.5000 24	0.500027(31)	0.500013(23)	$\frac{1}{2}$ [27]
TR-1,2	12	15	0.2902 67	0.290261(22)	0.290258(19)	0.295 [19]
TR-2	6	9	0.4999 85	0.499987(20)	0.499978(20)	$\frac{1}{2}$ [27]
TR-1	6	6	0.4999 93	0.499994(17)	0.499996(14)	$\frac{1}{2}$ [1, p. 17]

^a $L \leq 2048$

tion thresholds for neighbourhoods for fixed number z . For instance $\bar{p}_c(z=6)$ is the mean value of p_c for TR-1, TR-2, TR-3, TR-5 lattices, while $\bar{p}_c(z=30)$ is based on values of p_c for TR-1,2,3,4, TR-1,2,4,5, TR-1,3,4,5 and TR-2,3,4,5 lattices, respectively. Additionally, we checked the quality of such fits for the Galam–Mauger formula [36], which for fixed network topology reduces to the following power-law dependence

$$p_c \propto (z-1)^{-a}. \quad (8)$$

Unfortunately, the formulas $\bar{p}_c(z)$ describing the depen-

dence on z are not consistent with either (6) or (7) or (8). However, we notice that the maximum value of p_c for the fixed value of coordination number z follows a power law

$$\max_{z=\text{const}} p_c \propto z^{-\delta} \quad (9)$$

with the power $\delta \approx 0.811(20)$ (see Figure 3a).

As the combination of d and z seems to be insufficient to differentiate among various lattices with assumed neighbourhoods we are looking for another index ξ which may be useful for both: deriving a formula $p_c(\xi)$ and re-

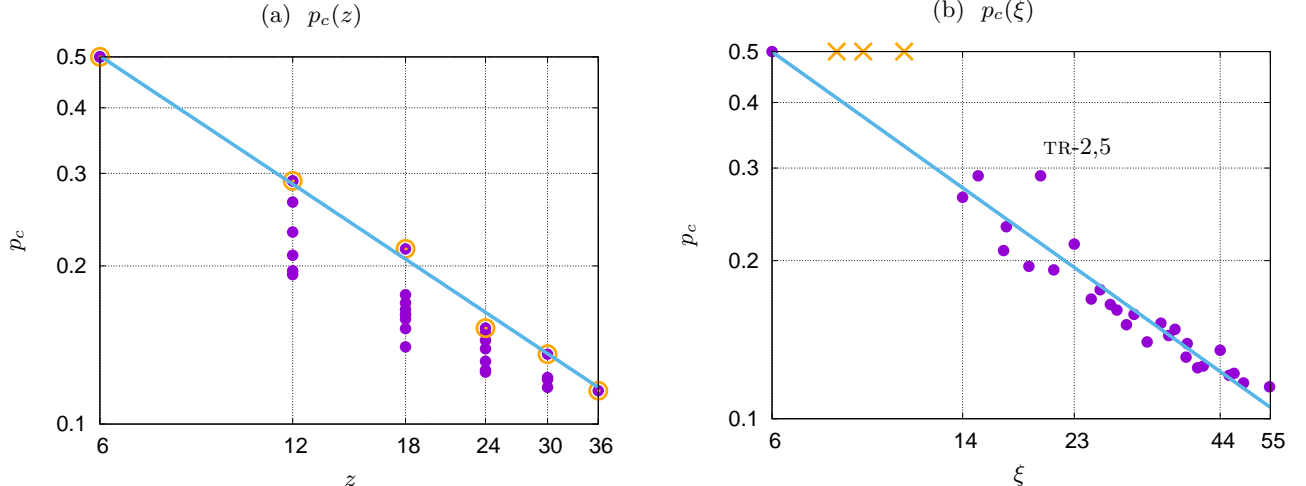


FIG. 3: (Color online). Percolation thresholds for complex neighbourhoods on triangular lattice. (a) Degenerated dependence of the percolation threshold p_c on the coordination number z . The maxima of p_c for fixed z follow Equation (9). The power is $\delta \approx 0.811$. (b) Power fit (11) of the percolation thresholds p_c vs. ξ for complex neighbourhoods. The exponent γ in Equation (9) is 0.705. The p_c values for equivalents of TR-1 neighbourhoods (marked with crosses) are excluded from fitting.

moving the p_c -degeneracy. The attempts for such index identification were undertaken also in graph theory (for topological invariants for trees [37]) and in organic chemistry (for molecular topological index [38–40]).

Here, we propose a weighted square distance r_i^2 of z_i sites in the given neighbourhood which belong to ζ_i -th coordination zone

$$\xi = \sum_i z_i r_i^2 / \zeta_i. \quad (10)$$

The values of ξ are presented in Table I.

For complex neighbourhoods the dependence $p_c(\xi)$ follows roughly a power-law

$$p_c \propto \xi^{-\gamma} \quad (11)$$

with $\gamma \approx 0.705(23)$, except of a single value of p_c for TR-2,5 (see Figure 3b). Please note that $p_c(\text{TR-1}) = p_c(\text{TR-2}) = p_c(\text{TR-3}) = p_c(\text{TR-5})$ are exactly the same and equal to $\frac{1}{2}$ as these neighbourhoods are equivalent to those described in Ref. 27. Thus p_c values for TR-2, TR-3, TR-5 neighbourhoods are excluded from fitting.

V. CONCLUSIONS

Concluding, in this paper we estimated percolation thresholds p_c for random site triangular lattice percolation and for neighborhoods containing sites from the first to fifth coordination zone. The estimated values of percolation thresholds are collected in Table I.

We note that the method Bastas *et al.* [32] allows (at least partially) to get rid of finite size effects. The minima of the pairwise difference λ function presented in

Table I are consistent with a five digit accuracy with the percolation threshold p_c obtained for infinite lattice according to Equation (5). The five digit accuracy seems to outperform by at least one order of magnitude practical requirements on experimenters in any field of science where percolation theory may be applied.

As the percolation thresholds $p_c(z)$ are multiply degenerated, we propose the weighted square distance ξ to differentiate among various neighbourhoods. This index seems to be effective in this respect (at least for neighbourhoods investigated here).

Finally, the $p_c(\xi)$ dependence follows roughly a power law (11). The deviation from this dependence is observed only for p_c estimated for TR-2,5 lattice. The obtained results may be useful in further searching for the empirical formula for percolation thresholds [41].

Appendix A: Supplementary material

In Figure A1 neighbourhoods containing sites from $\zeta = 5$ coordination zone are presented. In Figure A2 the mean largest cluster size $\langle S_{\max} \rangle$ vs. the number of occupied sites, normalized to the system size N are presented. Figure A3 shows the probability of belonging to the largest cluster $\langle P_{\max} \rangle$ vs. occupation probability p . Sums of the pairwise difference λ vs. the occupation probability p are presented in Figure A4. In Figure A5 finite size corrections to p_c are presented.

- [1] D. Stauffer and A. Aharony, *Introduction to Percolation Theory*, 2nd ed. (Taylor and Francis, London, 1994).
- [2] J. Wierman, “Percolation theory,” in *Wiley StatsRef: Statistics Reference Online* (American Cancer Society, 2014) pp. 1–9.
- [3] S. R. Broadbent and J. M. Hammersley, “Percolation processes: I. Crystals and mazes,” *Mathematical Proceedings of the Cambridge Philosophical Society* **53**, 629–641 (1957).
- [4] J. M. Hammersley, “Percolation processes: II. The connective constant,” *Mathematical Proceedings of the Cambridge Philosophical Society* **53**, 642–645 (1957).
- [5] J. E. Ramírez, C. Pajares, M. I. Martínez, R. Rodríguez Fernández, E. Molina-Gayosso, J. Lozada-Lechuga, and A. Fernández Téllez, “Site-bond percolation solution to preventing the propagation of *Phytophthora zoospores* on plantations,” *Physical Review E* **101**, 032301 (2020).
- [6] Q. Zhang, B.-Y. Zhang, B.-H. Guo, Z.-X. Guo, and J. Yu, “High-temperature polymer conductors with self-assembled conductive pathways,” *Composites Part B—Engineering* **192**, 107989 (2020).
- [7] L. Cheng, P. Yan, X. Yang, H. Zou, H. Yang, and H. Liang, “High conductivity, percolation behavior and dielectric relaxation of hybrid ZIF-8/CNT composites,” *Journal of Alloys and Compounds* **825**, 154132 (2020).
- [8] K. Malarz, S. Kaczanowska, and K. Kułakowski, “Are forest fires predictable?” *International Journal of Modern Physics C* **13**, 1017–1031 (2002).
- [9] B. Ghanbarian, F. Liang, and H.-H. Liu, “Modeling gas relative permeability in shales and tight porous rocks,” *Fuel* **272**, 117686 (2020).
- [10] W. Cao, L. Dong, L. Wu, and Y. Liu, “Quantifying urban areas with multi-source data based on percolation theory,” *Remote Sensing of Environment* **241**, 111730 (2020).
- [11] S. Bartolucci, F. Caccioli, and P. Vivo, “A percolation model for the emergence of the Bitcoin Lightning Network,” *Scientific Reports* **10**, 4488 (2020).
- [12] R. M. Ziff, “Percolation and the pandemic,” *Physica A: Statistical Mechanics and its Applications* **568**, 125723 (2021).
- [13] S. Dong, A. Mostafizi, H. Wang, J. Gao, and X. Li, “Measuring the topological robustness of transportation networks to disaster-induced failures: A percolation approach,” *Journal of Infrastructure Systems* **26**, 04020009 (2020).
- [14] M. Li, R.-R. Liu, L. Lü, M.-B. Hu, S. Xu, and Y.-C. Zhang, “Percolation on complex networks: Theory and application,” *Physics Reports* (2021), 10.1016/j.physrep.2020.12.003.
- [15] A. A. Saberi, “Recent advances in percolation theory and its applications,” *Physics Reports* **578**, 1–32 (2015).
- [16] H. L. Frisch, E. Sonnenblick, V. A. Vyssotsky, and J. M. Hammersley, “Critical percolation probabilities (site problem),” *Physical Review* **124**, 1021–1022 (1961).
- [17] P. Dean, “A new Monte Carlo method for percolation problems on a lattice,” *Mathematical Proceedings of the Cambridge Philosophical Society* **59**, 397–410 (1963).
- [18] P. Dean and N. F. Bird, “Monte Carlo estimates of critical percolation probabilities,” *Mathematical Proceedings of the Cambridge Philosophical Society* **63**, 477–479 (1967).
- [19] N. W. Dalton, C. Domb, and M. F. Sykes, “Dependence of critical concentration of a dilute ferromagnet on the range of interaction,” *Proceedings of the Physical Society* **83**, 496–498 (1964).
- [20] C. Domb and N. W. Dalton, “Crystal statistics with long-range forces: I. The equivalent neighbour model,” *Proceedings of the Physical Society* **89**, 859–871 (1966).
- [21] M. Gouker and F. Family, “Evidence for classical critical behavior in long-range site percolation,” *Physical Review B* **28**, 1449–1452 (1983).
- [22] K. Malarz and S. Galam, “Square-lattice site percolation at increasing ranges of neighbor bonds,” *Physical Review E* **71**, 016125 (2005).
- [23] S. Galam and K. Malarz, “Restoring site percolation on damaged square lattices,” *Physical Review E* **72**, 027103 (2005).
- [24] M. Majewski and K. Malarz, “Square lattice site percolation thresholds for complex neighbourhoods,” *Acta Physica Polonica B* **38**, 2191–2199 (2007).
- [25] Z. Xun, D. Hao, and R. M. Ziff, “Site percolation on square and simple cubic lattices with extended neighborhoods and their continuum limit,” *Physical Review E* **103**, 022126 (2021).
- [26] C. d’Iribarne, M. Rasigni, and G. Rasigni, “From lattice long-range percolation to the continuum one,” *Physics Letters A* **263**, 65–69 (1999).
- [27] K. Malarz, “Site percolation thresholds on triangular lattice with complex neighborhoods,” *Chaos* **30**, 123123 (2020).
- [28] Ł. Kurzawski and K. Malarz, “Simple cubic random-site percolation thresholds for complex neighbourhoods,” *Reports on Mathematical Physics* **70**, 163–169 (2012).
- [29] K. Malarz, “Simple cubic random-site percolation thresholds for neighborhoods containing fourth-nearest neighbors,” *Physical Review E* **91**, 043301 (2015).
- [30] M. Kotwica, P. Gronek, and K. Malarz, “Efficient space virtualisation for Hoshen–Kopelman algorithm,” *International Journal of Modern Physics C* **30**, 1950055 (2019).
- [31] M. E. J. Newman and R. M. Ziff, “Fast Monte Carlo algorithm for site or bond percolation,” *Physical Review E* **64**, 016706 (2001).
- [32] N. Bastas, K. Kosmidis, P. Giazitzidis, and M. Maragakis, “Method for estimating critical exponents in percolation processes with low sampling,” *Physical Review E* **90**, 062101 (2014).
- [33] V. Privman, “Finite-size scaling theory,” in *Finite size scaling and numerical simulation of statistical systems*, edited by V. Privman (World Scientific, Singapore, 1990) pp. 1–98.
- [34] N. Bastas, K. Kosmidis, and P. Argyrakis, “Explosive site percolation and finite-size hysteresis,” *Physical Review E* **84**, 066112 (2011).
- [35] S. C. van der Marck, “Universal formulas for percolation thresholds — Comment,” *Physical Review E* **55**, 1228–1229 (1997).
- [36] S. Galam and A. Mauger, “Universal formulas for percolation thresholds,” *Physical Review E* **53**, 2177–2181 (1996).

- [37] S. Piec, K. Malarz, and K. Kułakowski, “How to count trees?” *International Journal of Modern Physics C* **16**, 1527–1534 (2005).
- [38] I. Gutman, “Selected properties of the Schultz molecular topological index,” *Journal of Chemical Information and Computer Sciences* **34**, 1087–1089 (1994).
- [39] H. P. Schultz, “Topological organic chemistry. 1. Graph theory and topological indices of alkanes,” *Journal of Chemical Information and Computer Sciences* **29**, 227–228 (1989).
- [40] H. Wiener, “Structural determination of paraffin boiling points,” *Journal of the American Chemical Society* **69**, 17–20 (1947).
- [41] W. Lebrecht, P.M. Centres, and A.J. Ramirez-Pastor, “Empirical formula for site and bond percolation thresholds on Archimedean and 2-uniform lattices,” *Physica A: Statistical Mechanics and its Applications* **569**, 125802 (2021).

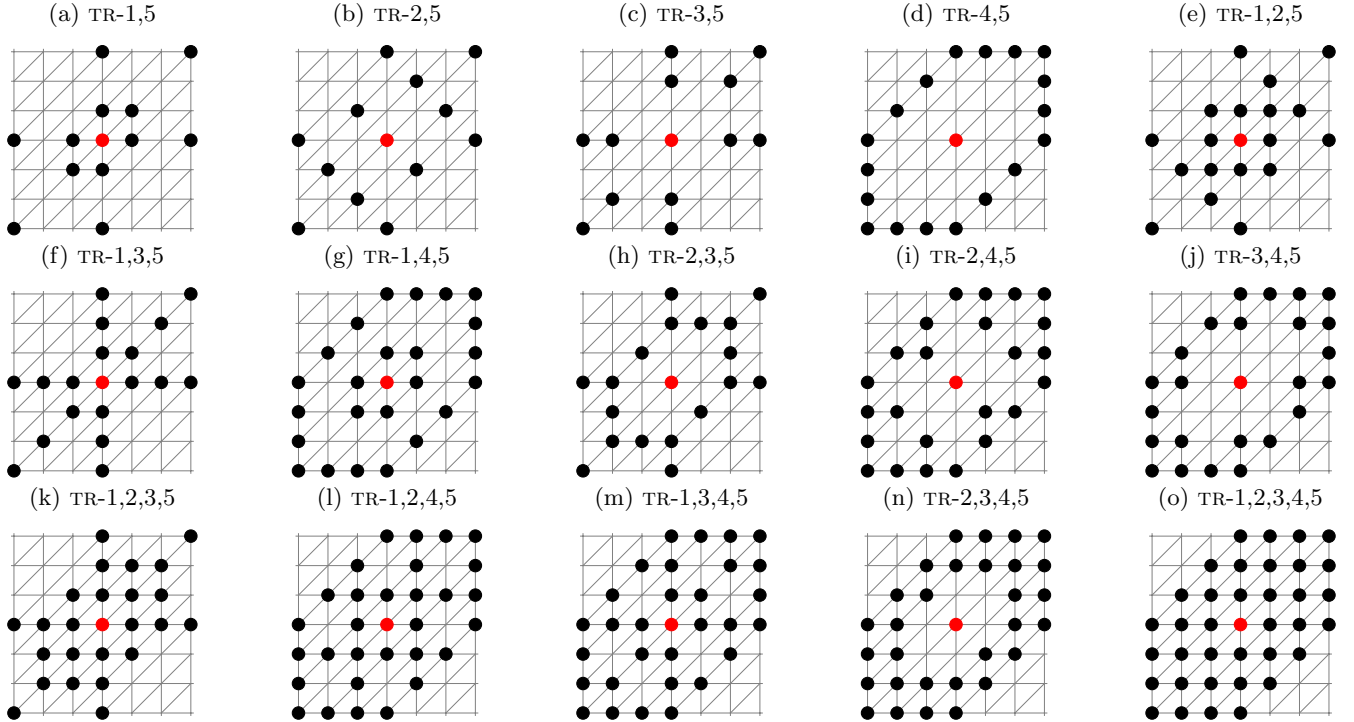
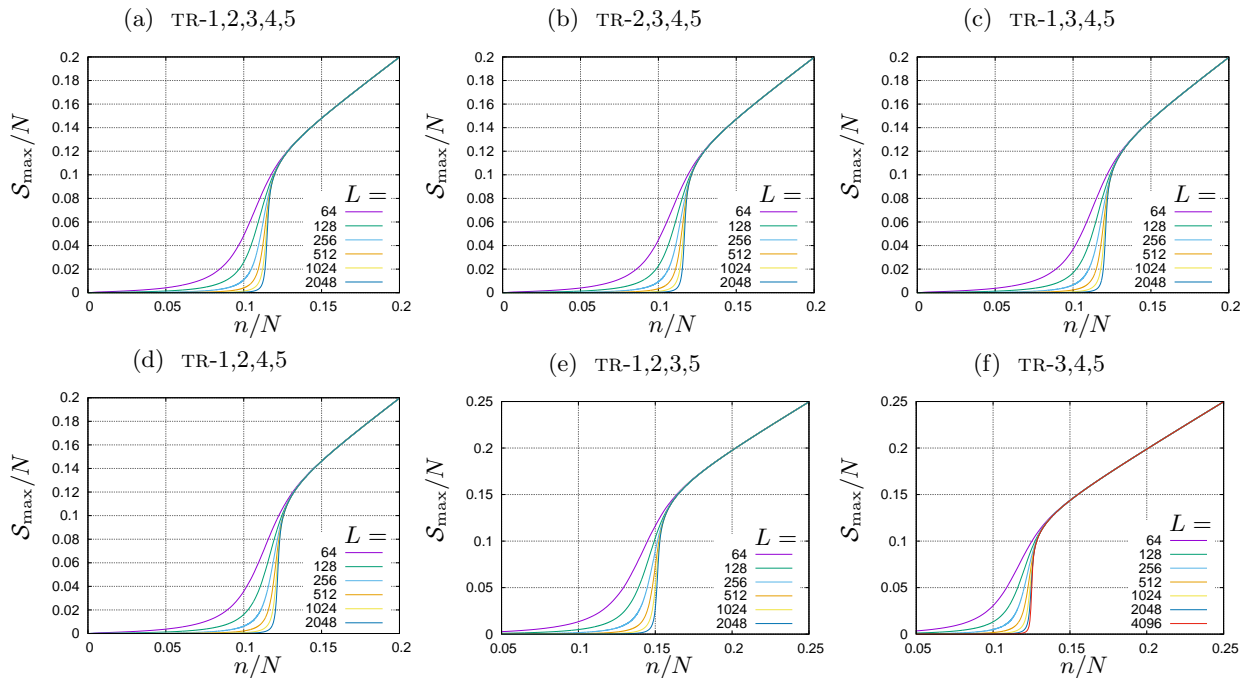
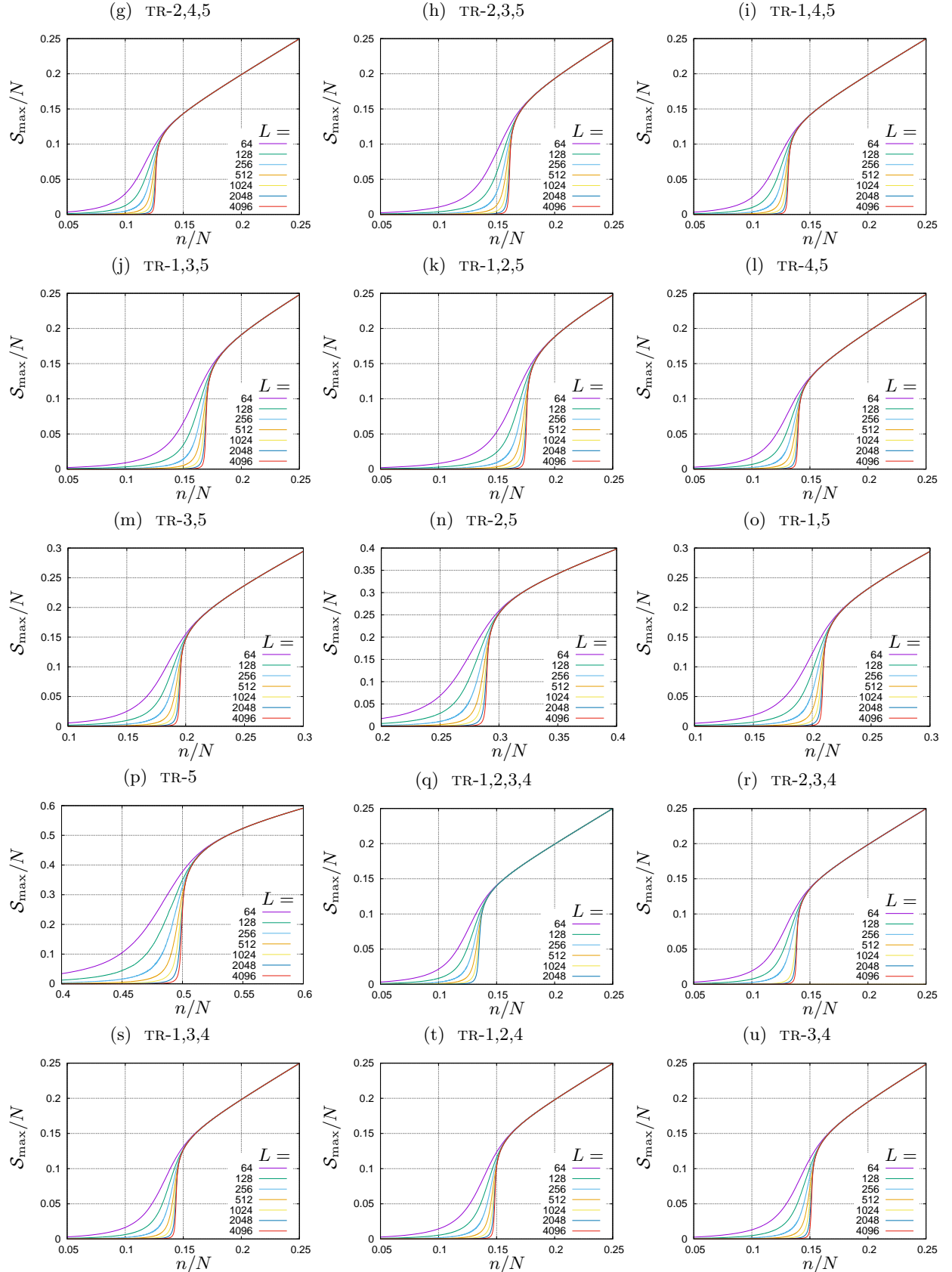


FIG. A1: Examples of neighborhoods containing the next-next-next-nearest neighbors on triangular lattice.





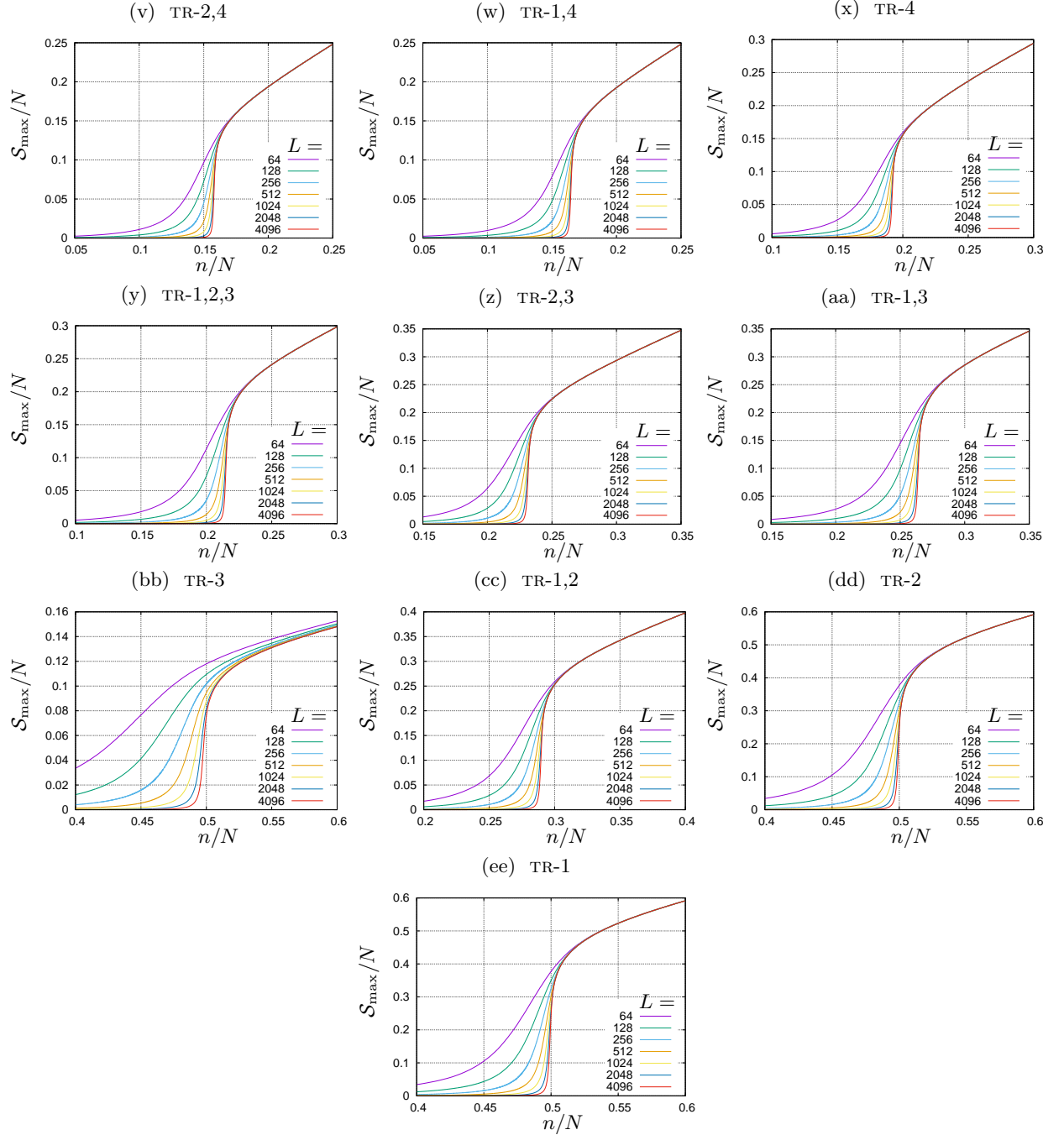
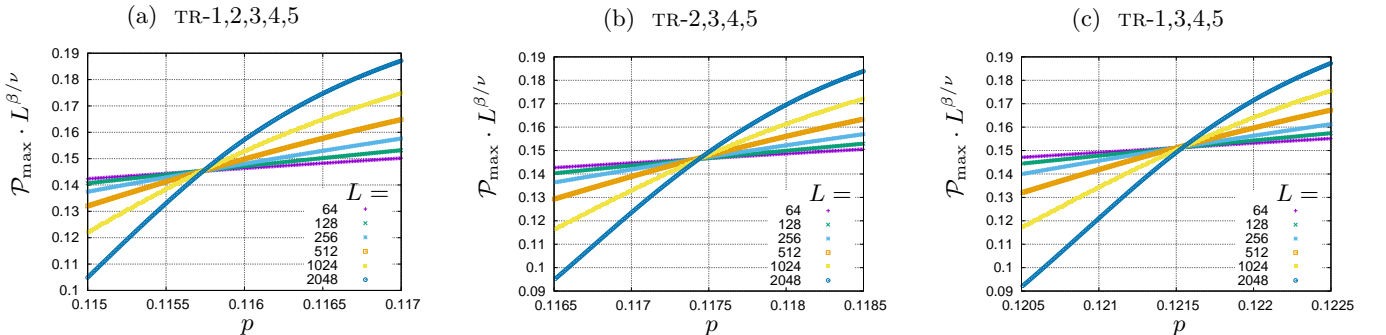
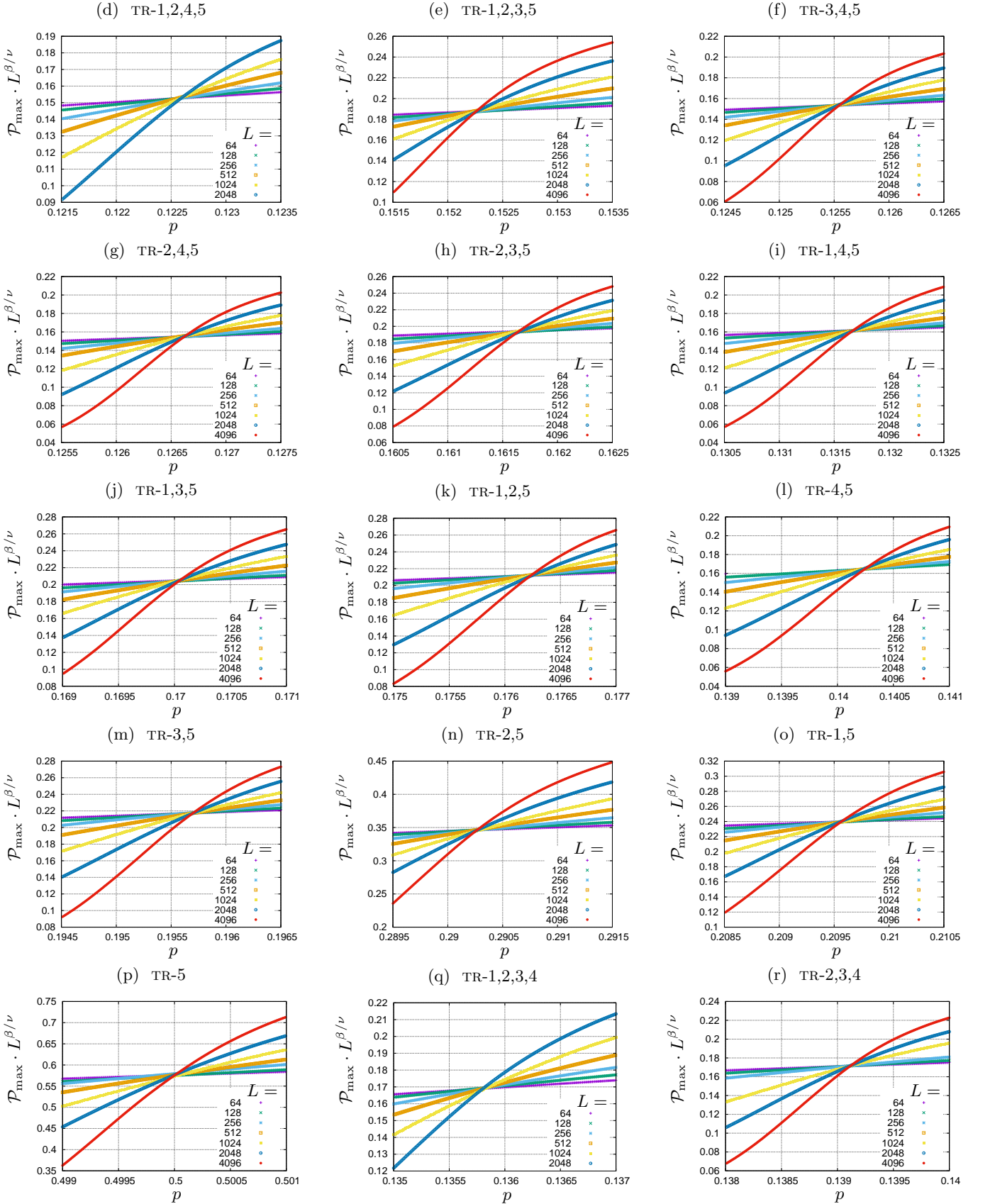


FIG. A2: Average the largest cluster size $\langle S_{\max} \rangle$ vs. number of occupied sites, both normalized to the system size N





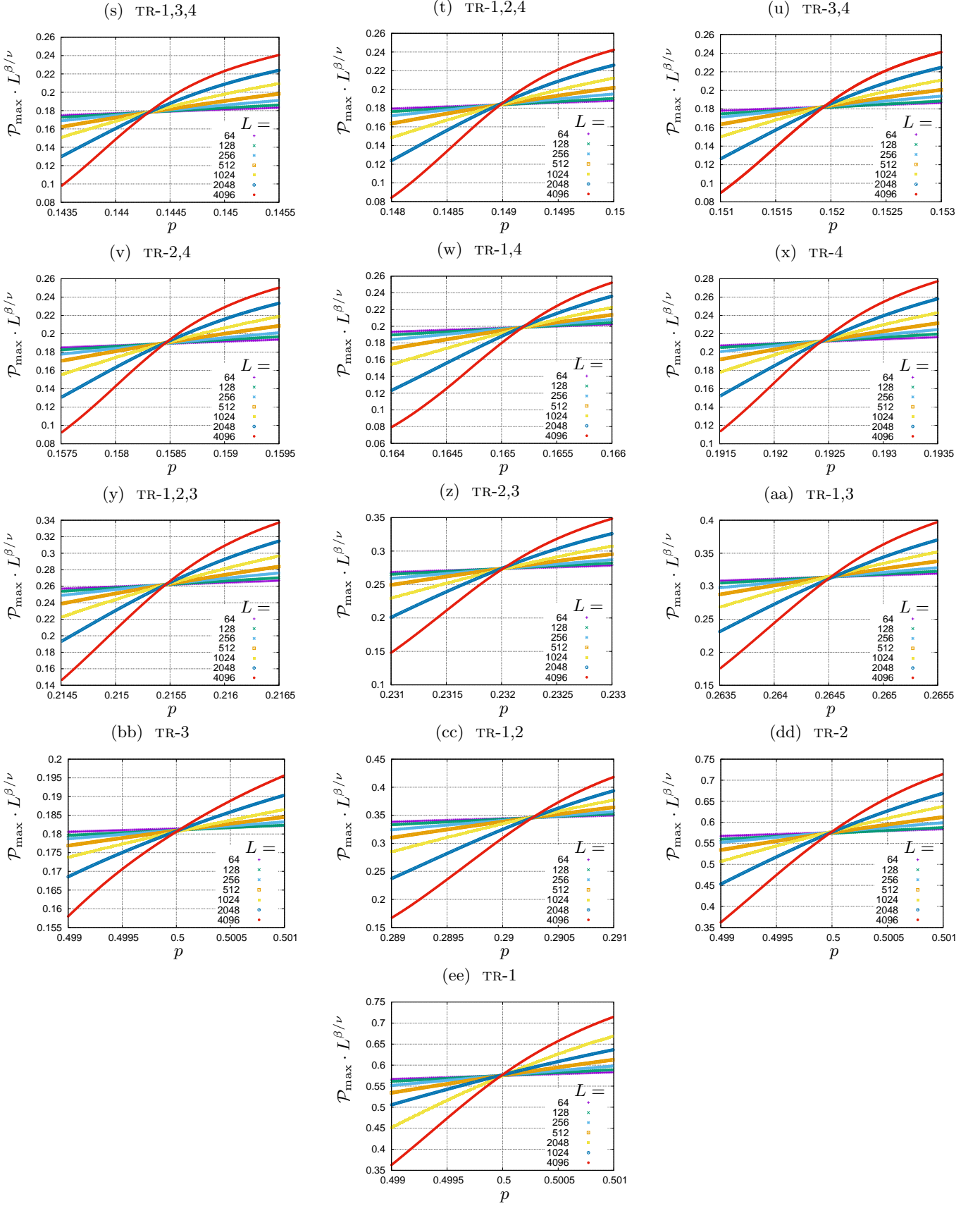
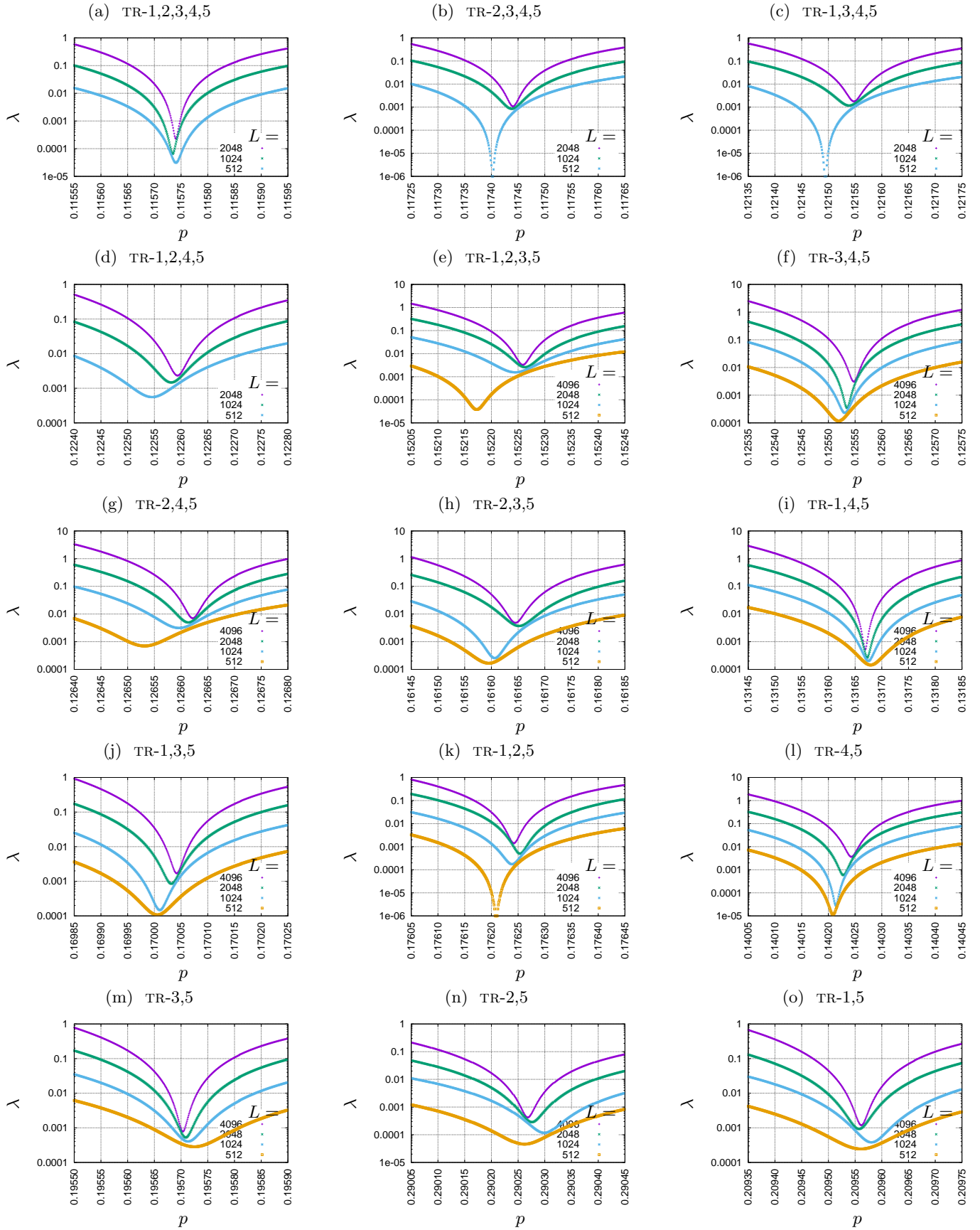
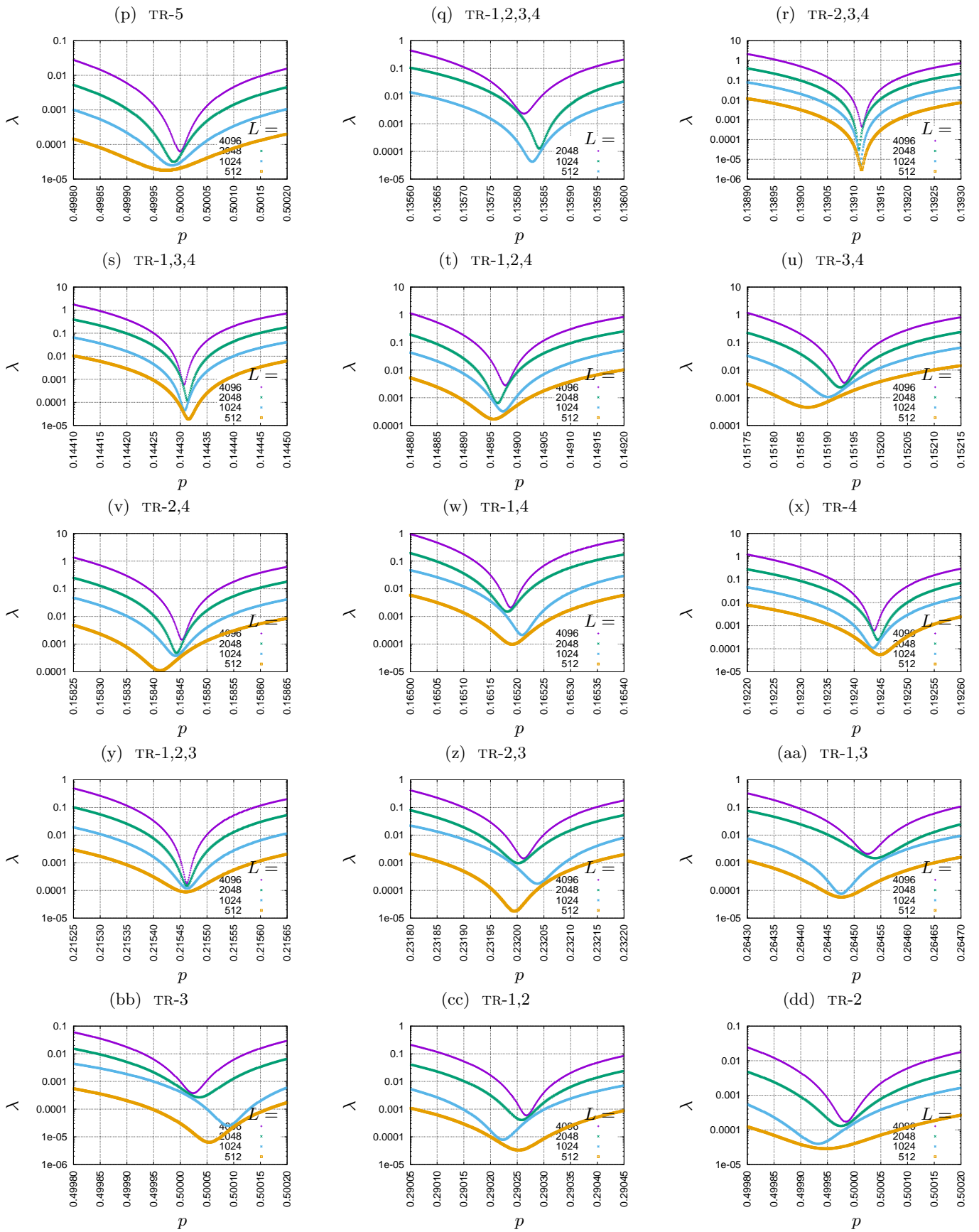
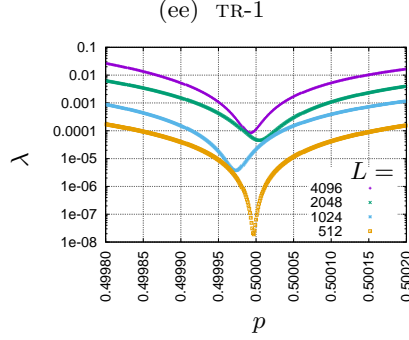
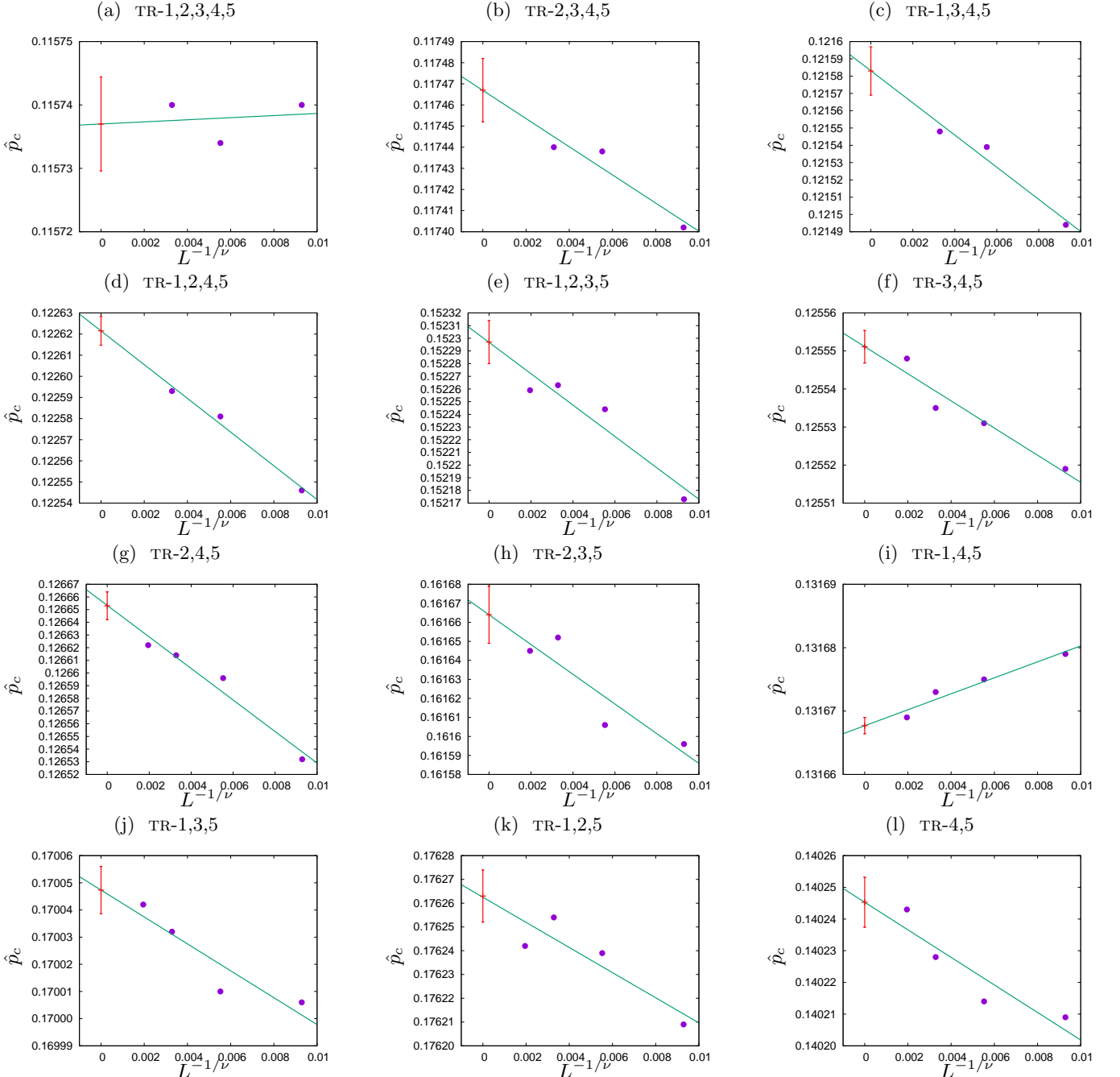
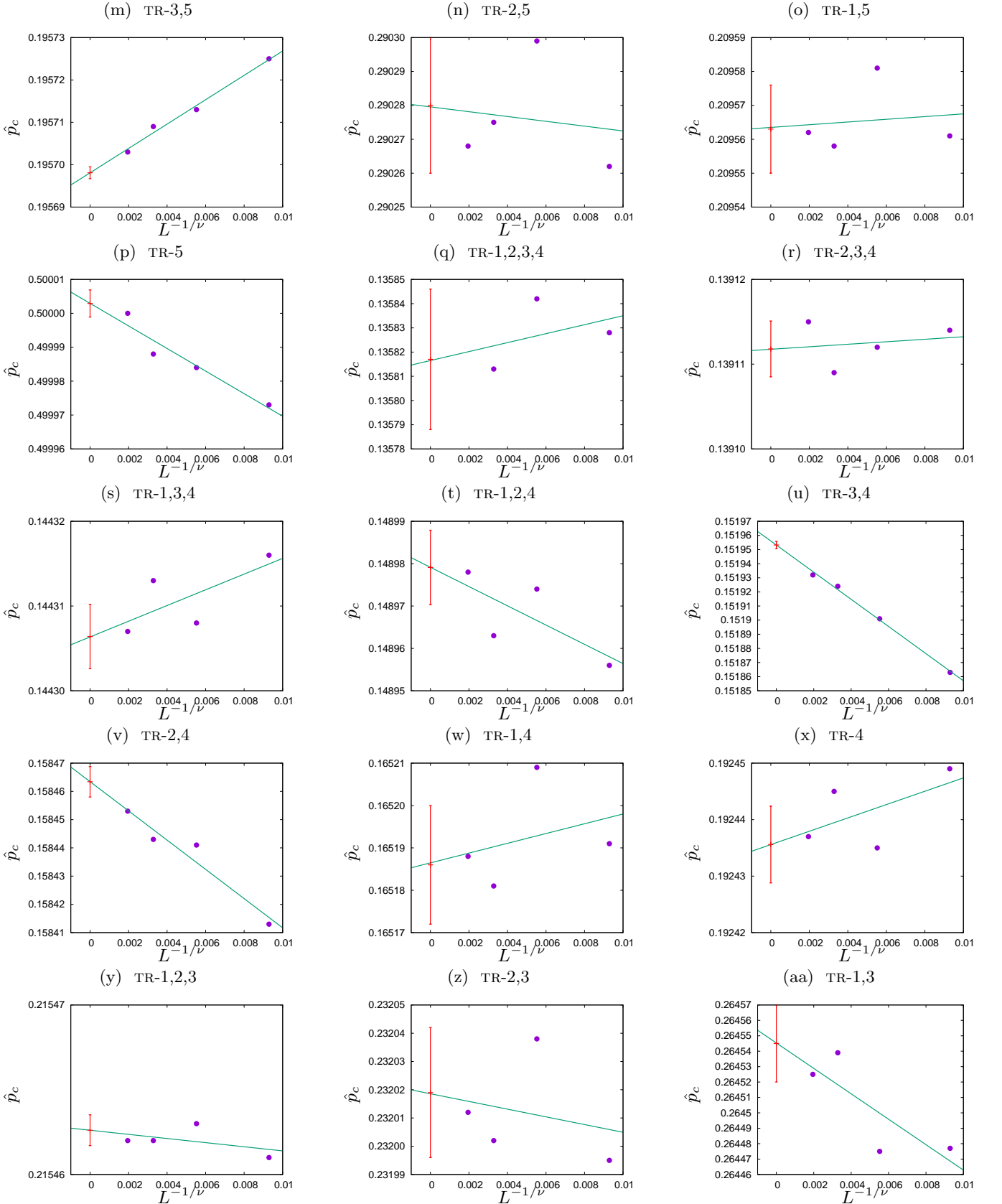


FIG. A3: Probability of belonging to the largest cluster $\langle \mathcal{P}_{\max} \rangle$ vs. occupation probability p





FIG. A4: Sum of pairwise differences $\langle \lambda \rangle$ vs. occupation probability p 



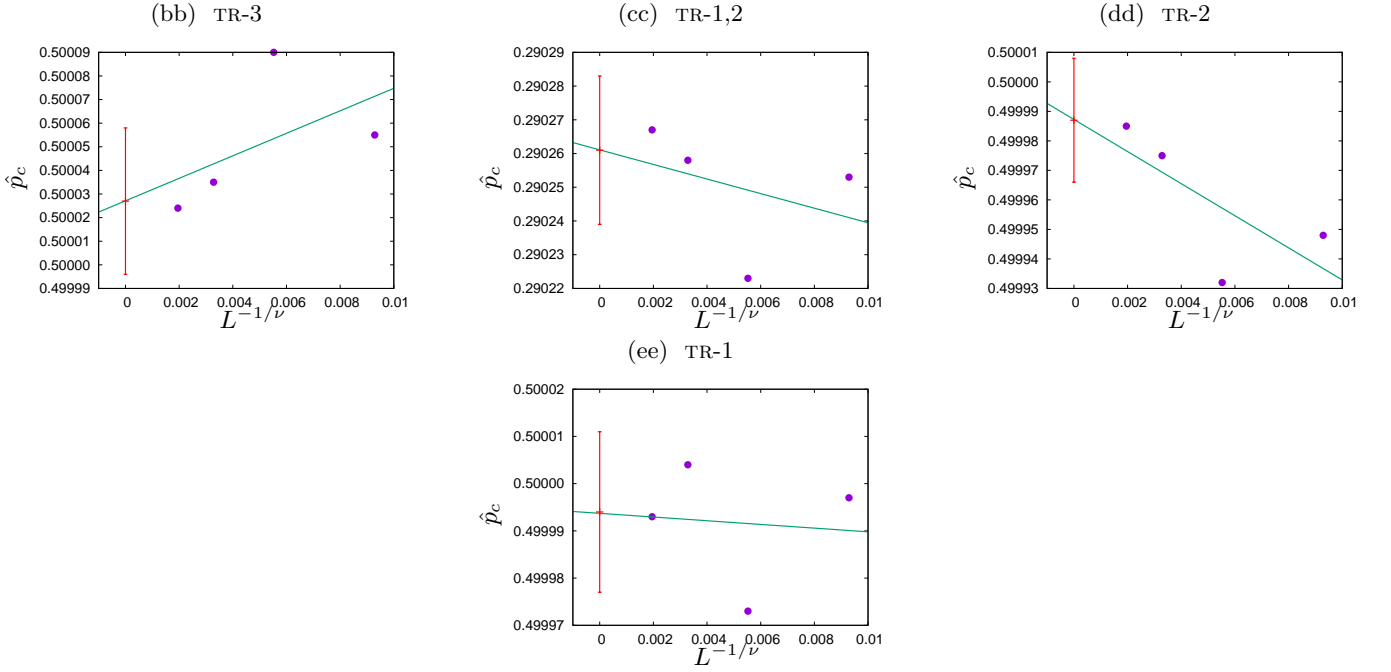


FIG. A5: Finite size effect corrections to p_c .